Journal of Sound and Vibration (2002) **250**(3), 465–483
doi:10.1006/jsvi.2001.3953, available online at http://www.idealibrary.com on IDEAL®

AN APPROACH TO PARAMETER IDENTIFICATION FOR A SINGLE-DEGREE-OF-FREEDOM DYNAMICAL SYSTEM BASED ON SHORT FREE ACCELERATION RESPONSE

N. JAKŠIĆ AND M. BOLTEŽAR

Faculty of Mechanical Engineering, University of Ljubljana, Aškerčeva 6, 1000 *Ljubljana, SI-Slovenia. E-mail: miha.boltezar@fs.uni-lj.si.*

(*Received* 4 *January* 2001, *and in final form* 9 *July* 2001)

An approach to parameter identification for the single-degree-of-freedom (s.d.o.f.) system is presented. It fits into the group of parametric system identification methods that use a structured mathematical model. It uses the free acceleration response of the system in order to estimate the parameters of the equation of motion for the model under consideration. The approach has been numerically tested on Duffing's oscillator with dry friction at different sampling rates of the acceleration time history and at different signal-to-noise ratios (SNR). The experiment has been carried out on an experimental device with the features of Duffing's oscillator. The validity and advantages of the approach are presented. The results show that this approach offers parameter identification with good quality for short time series using only a modest number of data points for a wide range of s.d.o.f. systems.

1. INTRODUCTION

In engineering practice, a good model of the real system or a few likely candidates for a good model of the real system are usually known or can be deduced from basic mechanical principles. The task is to determine the parameters of the model's equation of motion based on information contained in the system's dynamical response. There are several ways of identifying a model's parameters from the system's dynamical behaviour.

One study [1] considered the free vibrations of a single-degree-of-freedom (s.d.o.f.) system with combined viscous damping and Coulomb dry friction. This approach used only the amplitude decay of the displacement response of the system.

An approach to the parameter identification of assumed polynomials for the description of non-linearities in restoring and damping forces within a force dynamical system was used in reference [2]. This approach uses approximation theory with the polynomials of Tschebishev. The identification of a stable linear system using polynomial kernels was presented in reference [3]. An approach to the identification of modal damping parameters is discussed in reference [4].

Non-linear systems are approached in several different ways. The AVD model [5] offers a way of achieving parameter identification for a non-linear system by knowing the model and time series of displacement, velocity and acceleration. A method of parameter identification for a multi-input–multi-output model was also presented in reference [6]. A recursive approach for a class of non-linear systems from noisy measurements was introduced in reference [7]. An identification of weakly non-linear systems using equivalent

0022-460X/02/080465 + 19 $35.00/0

linearization was presented in reference [8]. A method used for estimations of the non-linear systems based on high order frequency–response functions was described in reference [9]. In references [10, 11], the Hilbert transform was used in order to identify the parameters of the s.d.o.f. non-linear system. The use of the wavelet transform entered the field of the non-linear system's parameter identification in reference [12]. Parameter identification via neural networks was presented in references [13–15]. The identification of a hysteretic system was studied in references [16–19].

In this paper, an approach to parameter identification is proposed that is simple, convenient for short measured time series and can be used on different classes of s.d.o.f. systems. Preliminary studies [20] have shown that the method gives very good results when phase-space variables are used for the identification and when the acceleration is the main source of the system's information [21].

Duffing's system with implemented dry friction was taken into consideration using its free acceleration response. The approach is studied numerically and is tested against a real experimental device. The approach is based on a geometrical representation of the solutions of the differential equation of motion. The solutions consist of a family of curves, but only one is realized with the given initial conditions. Each point on the realized solution and its time derivatives at a certain time satisfied the equation of motion. Hence, if the solution and its time derivatives are known, or somehow reconstructed, the differential equation of motion can be represented as an algebraic equation at that particular time if the parameters are considered to be unknowns. The procedure of reconstructing the velocity and displacement from the measured acceleration is presented and on this basis the parameters are estimated optimally in the least-squares sense.

2. THEORETICAL BASES OF THE APPROACH

It is not unusual in engineering practice to model a real dynamical system with a s.d.o.f. model in which the free vibrations are governed by equation (1). This can be a final model or just a first approach to the problem.

$$\ddot{x} - F(x, \dot{x}; a_1, \ldots, a_n) = 0, \tag{1}$$

where $a_1, \ldots, a_n$ represent n unknown parameters, which need to be determined. The approach is based on a geometrical representation of the solutions of the differential equation of motion. The solutions consist of a family of curves governed by two parameters. Only one trajectory is realized with the initial conditions. The differential equation of motion can be represented by an algebraic equation, where the parameters are considered to be unknowns. Hence, to estimate the n parameters of the equation of motion of the model, theoretically only n points on the trajectory and its time derivatives are needed. The problem is transformed into one of solving a system of algebraic equations or a pre-defined system of algebraic equations by means of a least-squares approximation, if there are more points than parameters.

The aim is to characterize a mechanical system with a chosen model. Consider that the type of differential equation of motion is known and the acceleration time history of the system under consideration is measured. Then the approach to a parameter identification can be divided into two parts:

1. *Reconstruction* of the state space; in other words, this is the reconstruction of the missing velocity and displacement time histories from the measured acceleration time

history by numerical integration. If the noise level contained in the measured time history is higher than $SNR \geqslant 40$ dB then smoothing of the latter has to be performed. In this paper, the approximating cubic splines were used for this purpose. For the case of low-level noise in the acceleration time history and for the case of an already-smoothed acceleration time history, the interpolation with splines of the third or fifth degree was used in order to numerically integrate the acceleration time history. For the case of a long measured time history (more than 2 cycles) the time-window approach is strongly recommended. The velocity time history obtained has to be interpolated and integrated again. The reconstruction phase of the approach is completely model independent.

2. *Estimation* of the parameters is achieved by a least-squares fit of the chi-squared merit function, equation (2), deduced from the equation of motion, equation (1). Since the equation of motion (1) is valid for any given time, the values of the equation for all the discrete times can be summed, and thus the merit function can be created as

$$\chi^2 = \sum_{i=1}^{m} [\ddot{x}_i - F(x_i, \dot{x}_i; a_1, \ldots, a_n)]^2, \tag{2}$$

where m denotes the number of points of the measured acceleration time history, $m > n$ and x_i, $\dot{x}_i$, $\ddot{x}_i$ denote displacement, velocity and acceleration at the ith sampling point respectively. $a_1, \ldots, a_n$ denote the n parameters to be identified. Because the velocity and displacement time histories have been numerically integrated from the acceleration time history, two new unknowns and a new variable are introduced. The two new unknowns are the free integration constants, i.e., the unknown initial conditions x_0 and $\dot{x}_0$. The new variable is the discrete time t_i at the ith sampling point. Hence, the merit function must be rewritten as

$$\chi^2 = \sum_{i=1}^{m} [\ddot{x}_i - F(x_i, \dot{x}_i, t_i; x_0, \dot{x}_0, a_1, \ldots, a_n)]^2. \tag{3}$$

The time-window approach requires segmentation of the original time history into sub-intervals. Each sub-interval is treated as a separate time history. A complete identification procedure is applied to each sub-interval and the results (identified parameters) are finally averaged over all sub-intervals. The time-window approach is necessary because of the numerical errors introduced by smoothing of the noisy acceleration time history and its double numerical integration.

3. DUFFING'S SYSTEM WITH DRY FRICTION

Duffing's system can be used for modelling dynamical systems with non-linear stiffness such as the post-buckling or large deflection of beams [22]. The dry friction is added to Duffing's system as the Coulomb model of dry friction. The equation of motion of free vibrations of Duffing's system with dry friction can be written as

$$\ddot{x} + a\dot{x} + bx + cx^3 + d\,\mathrm{sgn}(\dot{x}) = 0, \tag{4}$$

where a is a parameter which describes viscous damping, b is parameter representing the linear part of stiffness in the system, c denotes the non-linear part of stiffness and d is parameter which describes frictional force. In the case of free vibrations of a s.d.o.f. system,

the only attractor shapes possible are the point attractor and the limit cycle. The dynamical behaviour of the system under consideration is expected to be simple.

Applying the approach of parameter identification to Duffing's system with dry friction, equation (4), the chi-squared merit function can be rewritten as

$$\chi^2 = \sum_{i=1}^{m} [\ddot{x}_i + a(\dot{x}_i + \dot{x}_0) + b(x_i + x_0 + t_i\dot{x}_0) + c(x_i + x_0 + t_i\dot{x}_0)^3 + d\,\mathrm{sgn}(\dot{x}_i + \dot{x}_0)]^2, \quad (5)$$

where m denotes the number of points of measured acceleration time history, and t_i, x_i, $\dot{x}_i$, $\ddot{x}_i$ denote time, displacement, velocity and acceleration at the ith sampling point respectively. $a_1, \ldots, a_n$ denote the n parameters to be identified. Equation (5) results in a non-linear least-squares-fit problem. The non-linear-least-squares-fit problem was solved using the following iteration procedure:

1. The initial conditions must be guessed first. Thus, the non-linear least-squares-fit problem is transformed into a linear one. The choice of zero initial conditions worked well in all cases.
2. The linear least-squares-fit problem is solved.
3. The new value for the initial conditions is computed from the estimated regression parameters.
4. The second step is repeated until the convergence criterion is met.

The values of the parameters converge after a few steps of the iteration. In the case of the time-window approach, the estimated initial conditions from a certain time window are used as a good guess for the next time window if the time-window shift is not too big (which is rare).

4. NUMERICAL EXPERIMENT

The approach has been tested on Duffing's system with the Coulomb model of dry friction, (equation (4)). The default set of parameters were chosen as $a = 0{\cdot}2$, $b = 1$, $c = 0{\cdot}1$ and $d = 0$. The initial conditions were $x_0 = 1$ and $\dot{x}_0 = 0$. The equation of motion was numerically integrated using the Runge–Kutta method with an error estimation of $\mathcal{O}(h^5)$, were h denotes the constant integration step. The integration step was chosen as $h = 10^{-6}$ to minimize the integration error. This error was estimated to be between 10^{-19} and 10^{-15}. The numerically integrated acceleration time history was re-sampled and white noise of a certain level was added for further use. All of the analyses in this section were made on a 12·5 s time history, roughly two cycles of the system were defined with the default parameter set.

The behaviour of the approach was tested on a noise-polluted acceleration time history with signal-to-noise ratios of $SNR = 60$ and 20 dB and with discretization of the acceleration time history of $SPC = 20$ and 80, where SPC stands for samples per cycle. The validity of the approach was tested by varying parameter c, which describes the non-linear part of the stiffness, and by simultaneously varying the parameters a and d, which describe viscous and frictional damping, respectively, to determine the possibility of a successful distinction between the different mechanisms of energy dissipation.

The reconstruction with approximating cubic splines was used in order to smooth the noisy data and to define the function for reconstruction of the state space—the velocity and displacement time series.

4.1. THE INFLUENCE OF VARYING STIFFNESS NON-LINEARITY

Two distinct values of parameter c were used: 0·1 and 1. The results are presented in Table 1 for $c = 0{\cdot}1$ and Table 2 for $c = 1$. The sampling rate is presented in the first column denoted by *SPC*. The second column, denoted by Par., shows the names of the parameters. The third column, denoted by Val., defines the true values of the parameters in the second column. The next two groups of columns present the results estimated from the acceleration time history polluted with different levels of white noise denoted by *SNR*. Within each group the first column, denoted by est., presents the identified values of the parameters while the second column, denoted by err., gives the relative errors in %. The parameter d has not been identified in this subsection because its value is zero.

Tables 1 and 2 show the convergence of the estimated parameter's values towards the true values with increasing values of *SPC*. It can also be seen that the noise is detrimental to the

TABLE 1

Parameter identification results on 2 cycles of Duffing's system acceleration time history at different sampling rates and SNRs for $c = 0{\cdot}1$

			$SNR = 60$ dB		$SNR = 20$ dB	
SPC	Par.	Val.	est.	err. (%)	est.	err. (%)
20	a	0·2	0·1998	− 0·10	0·1841	− 7·95
	b	1·0	0·9998	− 0·02	0·9615	− 3·85
	c	0·1	0·1007	0·70	0·2204	> 100·00
	x_0	1·0	0·9994	− 0·06	0·9328	− 6·72
	y_0	0·0	0·0000	0·00	0·0065	—
80	a	0·2	0·1999	− 0·05	0·1887	− 5·65
	b	1·0	1·0000	0·00	0·9908	− 0·92
	c	0·1	0·1001	0·10	0·1330	33·00
	x_0	1·0	0·9997	− 0·03	0·9682	− 3·18
	y_0	0·0	0·0000	0·00	0·0082	—

TABLE 2

Parameter identification results on 2 cycles of Duffing's system acceleration time history at different sampling rates and SNRs for $c = 1$

			$SNR = 60$ dB		$SNR = 20$ dB	
SPC	Par.	Val.	est.	err. (%)	est.	err. (%)
20	a	0·2	0·1981	− 0·95	0·1704	− 14·80
	b	1·0	1·0141	1·41	0·9250	− 7·50
	c	1·0	0·9527	− 4·73	1·2151	21·51
	x_0	1·0	0·9755	− 2·45	0·8463	− 15·37
	y_0	0·0	− 0·0006	—	0·0124	—
80	a	0·2	0·1991	− 0·45	0·1876	− 6·20
	b	1·0	1·0109	1·09	0·9541	− 4·59
	c	1·0	0·9631	− 3·69	1·0949	9·49
	x_0	1·0	0·9789	− 2·11	0·9856	− 1·44
	y_0	0·0	0·0022	—	0·0107	—

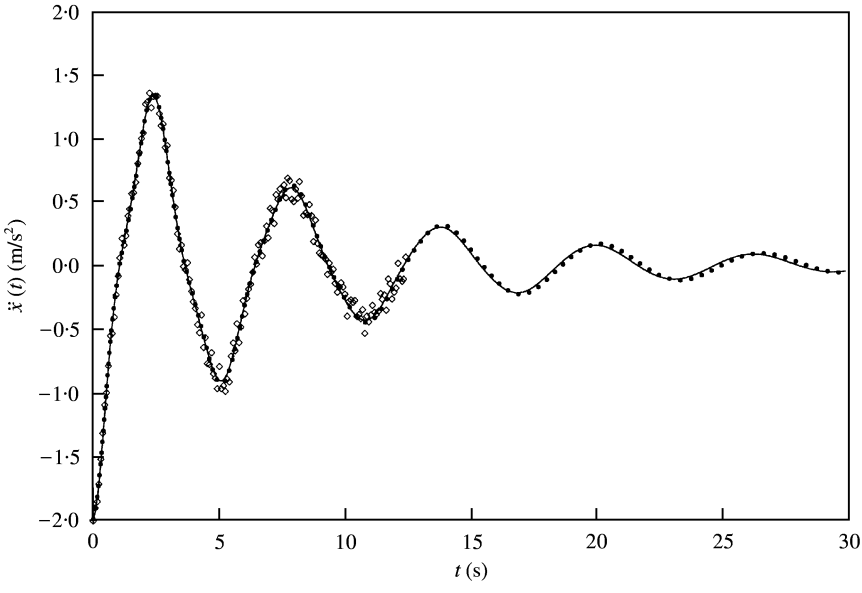

Figure 1. The acceleration response of Duffing's system with $c = 1$ based on the true values of the parameters (——), noisy data with $SNR = 20\,\text{dB}$ (◇), on which the identification has been performed, and the numerically integrated response based on the identified parameters (●).

quality of identification. Parameter b has the smallest relative errors. Hence, the system is more sensitive to a change in parameter b than to any of the other parameters. Because the lowest sensitivity is to parameter c, this parameter is the least accurately estimated. The relative errors of estimated parameter's values are generally well below 10%, except for the parameter c.

The comparison between the true response of the system and the response integrated from the estimated parameters is presented in Figure 1 for $c = 1$. The graph shows the acceleration response based on the true values of the parameters (—), noisy data with $SNR = 20\,\text{dB}$ (◇) and a numerically integrated response based on identified parameters (•). The figure corresponds to the parameters identified with $SNR = 20\,\text{dB}$ and $SPC = 80$ (Table 2). It can be seen that the true response and the response from the estimated parameters are almost indistinguishable.

4.2. THE POSSIBILITY OF A SUCCESSFUL DISTINCTION BETWEEN DIFFERENT MECHANISMS OF ENERGY DISSIPATION

Two combinations of parameters a and d were used: ($a = 0{\cdot}2$, $d = 0{\cdot}01$) and ($a = 0{\cdot}2$, $d = 0{\cdot}1$). The results are presented in Table 3 for $a = 0{\cdot}2$, $d = 0{\cdot}01$ and Table 4 for $a = 0{\cdot}2$, $d = 0{\cdot}1$. The configuration of the tables is the same as in the previous sub-section.

In Tables 3 and 4, the convergence of the estimated values of the parameters towards the true values with increasing values of SPC can be seen again. It can also be seen that the noise worsens the quality of identification.

Now concentrate on the part of the tables denoted with $SPC = 80$ and $SNR = 20\,\text{dB}$. The parameter d, which describes the dry friction, is always underestimated. The largest relative errors of the estimated parameters appear when the values of the different damping mechanisms are roughly of the same magnitude. In the case of the predominant influence of

TABLE 3

Parameter identification results on 2 cycles of Duffing's system acceleration time history at different sampling rates and SNRs for $a = 0{\cdot}2$, $d = 0{\cdot}01$

			$SNR = 60$ dB		$SNR = 20$ dB	
SPC	Par.	Val.	est.	err. (%)	est.	err. (%)
20	a	0·2	0·2001	0·05	0·1585	−20·75
	b	1·0	1·0037	0·37	0·9681	− 3·19
	c	0·1	0·0944	− 5·60	0·2094	>100·00
	d	0·01	0·0099	−1·00	0·0219	>100·00
	x_0	1·0	0·9970	− 0·30	0·9305	− 6·95
	y_0	0·0	0·0023	—	0·0089	—
80	a	0·2	0·1997	− 0·15	0·1923	− 3·85
	b	1·0	0·9995	−0·05	0·9913	− 0·87
	c	0·1	0·0997	− 0·30	0·1320	32·00
	d	0·01	0·0098	− 2·00	0·0080	− 20·00
	x_0	1·0	0·9994	− 0·06	0·9694	− 3·06
	y_0	0·0	0·0003	—	0·0083	—

TABLE 4

Parameter identification results on 2 cycles of Duffing's system acceleration time history at different sampling rates and SNRs for $a = 0{\cdot}2$, $d = 0{\cdot}1$

			$SNR = 60$ dB		$SNR = 20$ dB	
SPC	Par.	Val.	est.	err. (%)	est.	err. (%)
20	a	0·2	0·2545	27·25	0·2703	35·15
	b	1·0	1·0717	7·17	1·1794	17·94
	c	0·1	− 0·0352	< −100·00	− 0·0319	< −100·00
	d	0·1	0·0867	−13·30	0·0727	−27·30
	x_0	1·0	1·0135	1·35	0·9184	− 8·16
	y_0	0·0	0·0149	—	0·0249	—
80	a	0·2	0·2292	14·00	0·2732	36·60
	b	1·0	1·0793	7·93	1·0267	2·67
	c	0·1	− 0·0117	< −100·00	0·0073	− 92·70
	d	0·1	0·0921	− 7·90	0·0752	− 24·80
	x_0	1·0	1·0038	0·38	1·0529	5·29
	y_0	0·0	− 0·0019	—	− 0·0084	—

viscous damping, the results are estimated slightly better than in the opposite case. Generally, the parameter a (viscous damping) is estimated better than the parameter d (dry friction). Parameter b again experiences the smallest relative errors, around or below 2%, due to the system's higher sensitivity to any change in b. The parameter c is the least accurately estimated, between 30 and 90%, due to the dynamical system having the lowest sensitivity to the parameter c at its value of 0·1. This means that the more the dynamical response of the system is influenced by a certain parameter, the more accurately its value can be determined from the response. Tables 1 and 2 show that the influence of parameter

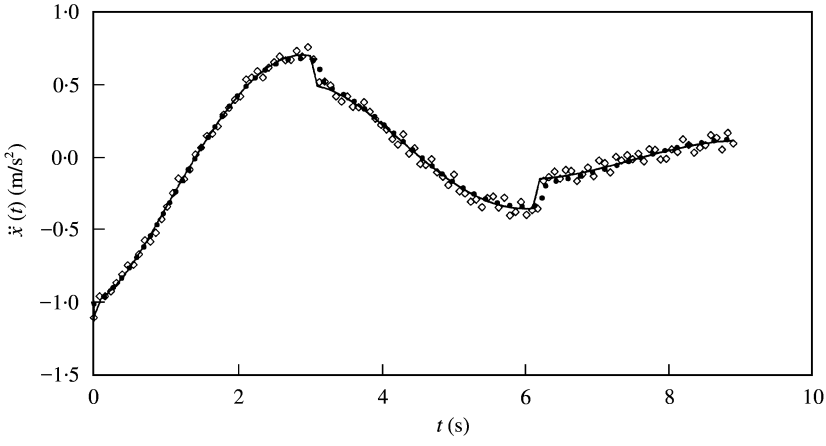

Figure 2. The acceleration response of Duffing's system with ($a = 0{\cdot}2$, $d = 0{\cdot}1$) based on the true values of the parameters (——), noisy data with $SNR = 20$ dB (◇), on which the identification has been performed, and the numerically integrated response based on the identified parameters (●).

c on the system's response is increased if the absolute value of the parameter is increased. In that case, the identification is more successful.

The comparison between the true response of the system and response integrated from estimated parameters is presented in Figure 2 for the most unfavourable scenario ($a = 0{\cdot}2$, $d = 0{\cdot}1$). The graph shows the acceleration response based on the true values of the parameters (—), noisy data with $SNR = 20$ dB (◇) and numerically integrated response based on identified parameters (•). Figure 2 corresponds to parameters identified with $SNR = 20$ dB and $SPC = 80$ (Table 4). It can be seen that the true response and the response from the estimated parameters are very similar. The largest differences can be seen at the acceleration jump at amplitudes, mainly due to the continuous nature of the splines and the non-continuous nature of the Coulomb model of dry friction.

5. COMPARISON BETWEEN REFERENCE [12] AND THE APPROACH IN THIS PAPER

Staszewski developed an identification method for non-linear systems based on multi-scale ridges and skeletons of the wavelet transform [12]. Here, Duffing's system with dry friction was used with zero viscous damping, the values of the parameters were the same as in reference [12]: $a = 0$, $b = 1{\cdot}579$, $c = 100$ and $d = 1{\cdot}3 \times 10^{-3}$. The Gaussian noise was added in % of the maximum amplitude value. In order to reconstruct the state space, the approximating cubic splines were used again. The parameter a was not included because its value is zero.

The results of the reference method [12] and the approach in this paper are presented in Table 5. In the first column, Par., are the names of the parameters. The second column, Val., defines the true values of the parameters in the first column. The third column shows the methods used for the identification. *Wavelet* is the method from reference [12], *Case* (a) denotes the present approach using the same signal parameters as reference [12]: time duration = 120 s, samples = 231, time step = 0·52083 s, which gives roughly 8·8 samples per cycle, and *Case* (b) where the signal parameters are adjusted to the needs of the approach: time duration = 12 s, samples = 230, time step = 0·052083 s, which gives roughly 88

TABLE 5

Comparison between the method in reference [12] *and the present approach*

Par.	Val.	Method	Noise 0%	Noise 5%	Noise 10%	Noise 20%
		Wavelet	1·586	1·590	1·578	1·584
b	1·579	*Case* (a)	1·568	1·597	1·672	1·790
		Case (b)	1·583	1·580	1·584	1·610
		Wavelet	97·0	96·3	96·9	106·7
c	100·0	*Case* (a)	103·8	93·3	71·1	7·6
		Case (b)	99·4	99·7	98·7	93·9
		Wavelet	$1{\cdot}296 \times 10^{-3}$	$1{\cdot}320 \times 10^{-3}$	$1{\cdot}296 \times 10^{-3}$	$1{\cdot}238 \times 10^{-3}$
d	$1{\cdot}3 \times 10^{-3}$	*Case* (a)	$1{\cdot}289 \times 10^{-3}$	$1{\cdot}364 \times 10^{-3}$	$1{\cdot}415 \times 10^{-3}$	$-1{\cdot}451 \times 10^{-2}$
		Case (b)	$1{\cdot}230 \times 10^{-3}$	$1{\cdot}251 \times 10^{-3}$	$1{\cdot}331 \times 10^{-3}$	$1{\cdot}521 \times 10^{-3}$

samples per cycle. *Case* (b) has one-tenth the duration time and a ten times higher sampling frequency. However, all three methods have the same number of samples. Then the next four columns present the results estimated from the acceleration time history polluted with different levels of Gaussian noise. The designation of noise levels corresponds to that used in reference [12].

Table 5 shows that the results of this approach and the reference method are in very good agreement if the input time history is prepared for this approach, i.e., if the sampling frequency is high enough. The method appears to be workable on shorter signals, implements initial conditions and is easier to implement.

6. EXPERIMENT

The experimental work was undertaken on an experimental device made for the purpose which resembles the features of Duffing's oscillator by allowing high-amplitude oscillations. The first task was the comparison of the system's spring characteristic determined by a static test and estimated from the measured acceleration response of the system. In this case, no dry friction was present. The second task was the determination of, and distinction between, the equivalent viscous and friction damping of the system.

6.1. EXPERIMENTAL DEVICE

The experimental device is composed of two parallel but separated leaf springs clamped at one end and attached to an inertial mass at the other end. The dimensions of the spring's cross-section are $a \times h = 1\,\text{mm} \times 30\,\text{mm}$ and the spring's length is $l = 512\,\text{mm}$. The springs are separated by $e = 38\,\text{mm}$. Each spring has a mass of $m_s = 119{\cdot}1\,\text{g}$. The inertial mass is $m_i = 1{\cdot}892\,\text{kg}$. The complete inertial mass is estimated to be $m_c = m_i + 2m_s/3 = 1{\cdot}971\,\text{kg}$. The experimental device is shown in Figure 3.

6.2. DETERMINATION OF THE SPRING CHARACTERISTIC

The spring characteristic was first determined with a static test and then with the identification of Duffing's model parameters based on the measured acceleration response.

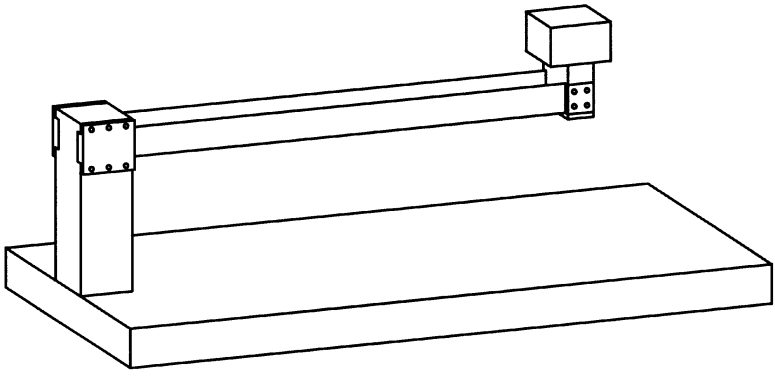

Figure 3. Experimental device.

6.2.1. *Static determination of the spring characteristic*

The statically measured spring characteristic was approximated with the linear equation (6), and the cubic equation (7), functions. The linear and cubic approximations of the measured spring characteristic are shown in Figure 4. The characteristic of the spring was experimentally confirmed to be an odd function, but only positive values are shown in Figure 4. The value of the coefficient k_1 of the characteristic equation (6) is $k_1 = 71{\cdot}172\,\mathrm{N/m}$. The values of the coefficients k_1 and k_3 of the characteristic equation (7) are $k_1 = 78{\cdot}072\,\mathrm{N/m}$ and $k_3 = -2470{\cdot}504\,\mathrm{N/m^3}$.

$$F(x) = k_1 x, \qquad F(x) = k_1 x + k_3 x^3, \tag{6, 7}$$

If k_1 and k_3 are divided by the total inertial mass, they fit to the parameters of Duffing's model b and c respectively. The value of b is computed as $b = k_1/m_c = 39{\cdot}610$ and $c = k_3/m_c = -1253{\cdot}427$.

6.2.2. *Dynamic determination of the spring characteristic*

The system was tested over a weakly non-linear range as seen in Figure 4.

The equivalent viscous damping ratio was estimated by using the logarithmic decrement of the linear model approach. The damping ratio δ was estimated to have a value of $\delta = 8{\cdot}694 \times 10^{-4}$ or in terms of Duffing's model, equation (4): $a = 1{\cdot}0943 \times 10^{-2}$.

The dynamically determined spring characteristic was computed by using the approach described in this paper. The acceleration time history was measured by an accelerometer glued to the inertial mass. The time history was sampled with a 12 bits A/D converter and stored on a PC HDD. The sampling frequency was set at 1 kHz. The measured acceleration is presented in Figure 5 (solid line).

The state space was reconstructed by the cubic spline interpolation because of the low noise contamination of the measured time history. The parameters were identified on the first 10 cycles of the response. The time-window approach to identification was adopted because of the length of the identification interval.

The impacts of variations of the length of the time-window, the sampling frequency and the step of the time-window shift on the validity of the estimated parameters were studied. The time history was re-sampled at 100 Hz and this is set to be the default sampling frequency. The default time-window length was set to two cycles and the default time-window shift was set to one-tenth of the cycle.

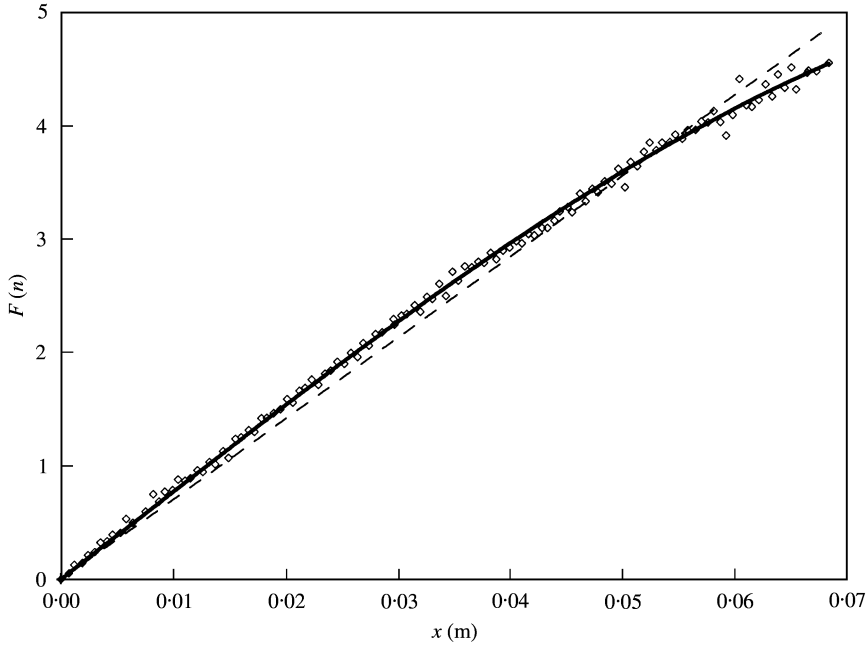

Figure 4. Statically determined spring characteristic: measurement points (◇), approximate linear characteristic (– – –) and approximate non-linear characteristic (——).

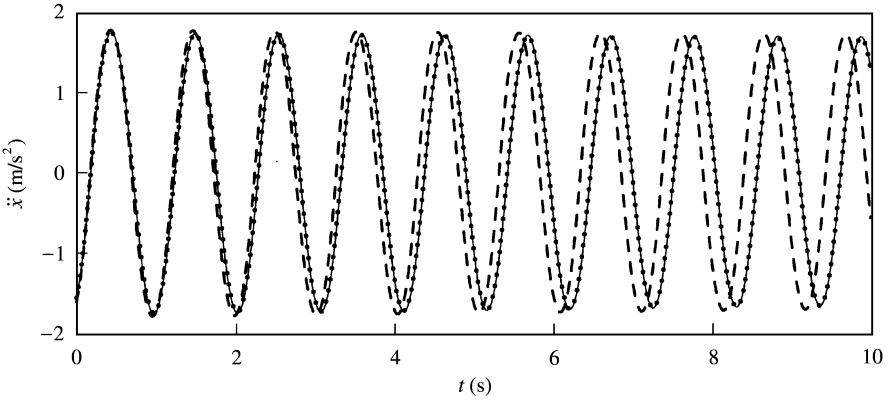

Figure 5. The comparison of the measured acceleration (——) with the Duffing's model response based on identified parameters from the approach in this paper (· · · · ·) and based on the static test and logarithmic decrement (– – –).

Influence of time-window length variation. The results of the identified parameters for varying time-window length are shown in Table 6. The first column has the chosen time-window lengths, the second column denotes the labels of the curve in Figure 6 and the last three columns contain values of the identified parameters of Duffing's model.

A detail of the 10 positive amplitude is shown in Figure 6. The measured acceleration is drawn with a thicker line and the acceleration responses of Duffing's model are drawn with thinner lines. The labels of the model responses correspond to the labels in Table 6.

It can be seen that the best choices for the length of the time window lie between 1 and 2 cycles (see Figure 6).

TABLE 6

Estimated values of the parameters of Duffing's model at different time-window lengths

Time-window length	Curve in Figure 6	a	b	c
0·5 cycle	ⓐ	$-8{\cdot}409\times10^{-3}$	37·078	−451·256
1 cycle	ⓑ	$1{\cdot}232\times10^{-2}$	36·778	−442·403
1·5 cycle	ⓒ	$1{\cdot}153\times10^{-2}$	36·686	−387·403
2 cycles	ⓓ	$1{\cdot}209\times10^{-2}$	36·283	−162·403
3 cycles	ⓔ	$1{\cdot}427\times10^{-2}$	36·287	−212·612
4 cycles	ⓕ	$1{\cdot}537\times10^{-2}$	36·250	−234·609
5 cycles	ⓖ	$2{\cdot}069\times10^{-2}$	35·932	−221·224

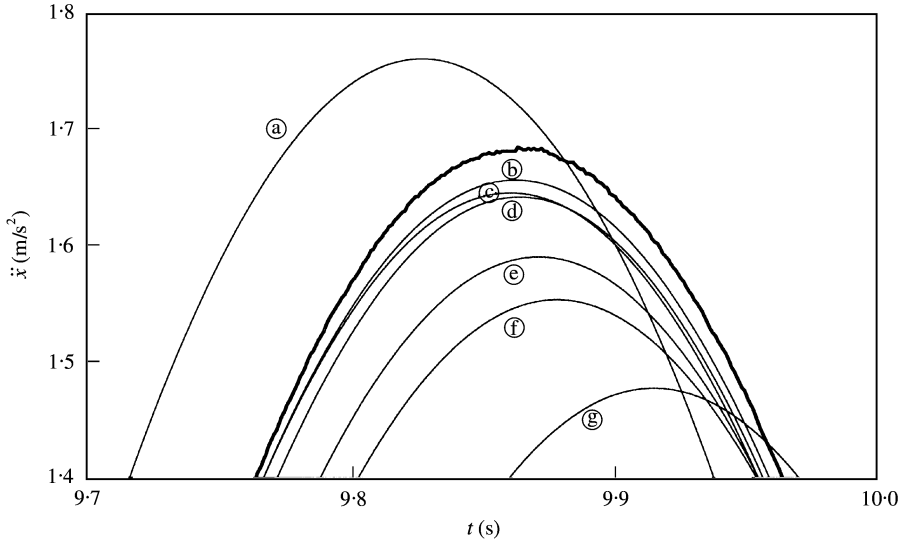

Figure 6. Measured acceleration of the experimental set-up (——) and simulated responses of Duffing's model for the parameters identified at different time-window lengths. For labels, see Table 6. Details of the 10th positive amplitudes.

TABLE 7

Estimated values of the parameters of Duffing's model at different sampling rates

Sampling rate	Curve in Figure 7	a	b	c
10 Hz	ⓐ	$1{\cdot}227\times10^{-2}$	36·291	−159·511
100 Hz	ⓑ	$1{\cdot}209\times10^{-2}$	36·283	−162·403
1000 Hz	ⓒ	$1{\cdot}188\times10^{-2}$	36·169	−157·292

Influence of sampling-rate variation. The results for parameters at various sampling rates are shown in Table 7. The first column lists the sampling rates, the second column indicates the label of the curve in Figure 7 and the last three columns contain values of the identified parameters of Duffing's model. The measured time history of the acceleration was re-sampled to match the desired sampling rate.

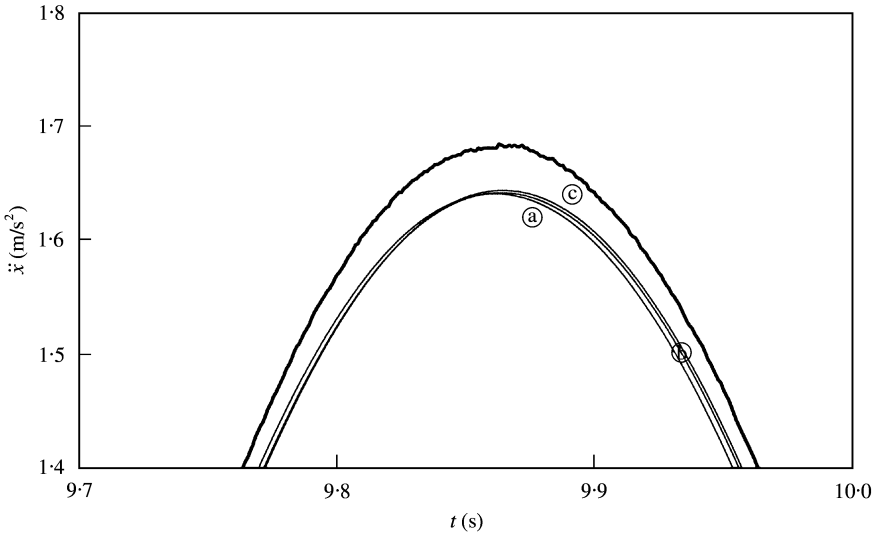

Figure 7. Measured acceleration of the experimental set-up (▬) and the simulated responses of Duffing's model for parameters identified at different sampling rates. For labels, see Table 7. Details of the 10th positive amplitudes.

TABLE 8

Estimated values of the parameters of Duffing's model at different time-window shifts

Time-window shift	Curve in Figure 8	a	b	c
$\frac{1}{100}$ cycle	ⓐ	$1{\cdot}029 \times 10^{-2}$	36·690	− 496·632
$\frac{1}{10}$ cycle	ⓑ	$1{\cdot}209 \times 10^{-2}$	36·283	− 162·403
1 cycle	ⓒ	$1{\cdot}055 \times 10^{-2}$	36·169	− 95·593

A detail of the 10th positive amplitude is shown in Figure 7. The measured acceleration is drawn with a thicker line and the acceleration responses of Duffing's model are drawn with thinner lines. The labels of the model responses correspond to the labels in Table 7.

Figure 7 shows that there are no major differences between the different sampling rates.

Influence of time-window shift variation. The results for parameters at various time-window shifts are shown in Table 8. The first column lists the chosen time-window shift, the second column indicates the label of the curve in Figure 8 and the last three columns contain values of the identified parameters of Duffing's model.

The details of the 10th positive amplitudes are shown in Figure 8. The measured acceleration is drawn with a thicker line and the acceleration responses of Duffing's model are drawn with thinner lines. The labels of the model responses correspond to the labels in Table 8.

Figure 8 shows that there are no major differences between the different time-window shifts.

The best possible combination of sampling rate (1000 Hz), time-window length (1 cycle) and time-window shift (1/1000 cycle) applied to the identification procedure on the measured

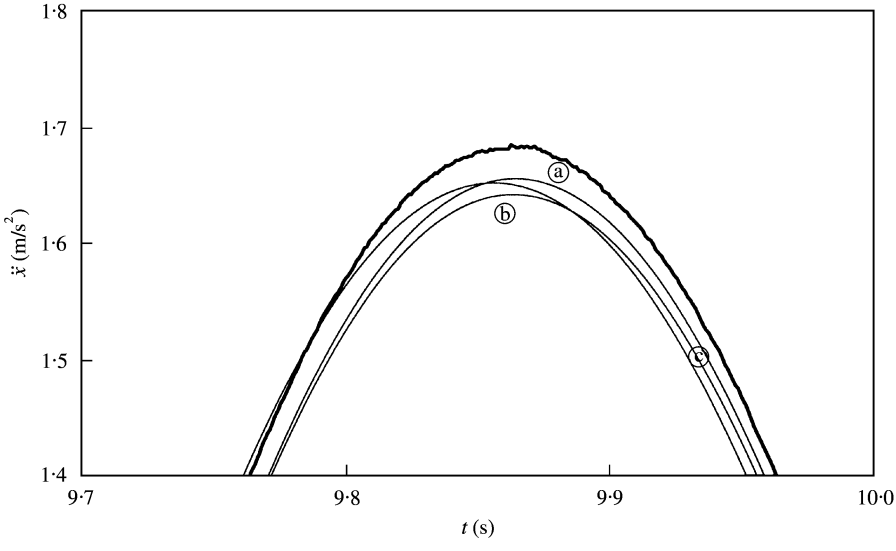

Figure 8. Measured acceleration of the experimental set-up (——) and the simulated responses of Duffing's model for parameters identified at different time-window shifts. For labels see Table 8. Details of the 10th positive amplitudes.

TABLE 9

Comparison of the statically and dynamically estimated values of the parameters of Duffing's model

Analysis	a	b	c
Static test		39·610	−1253·427
Logarithmic decrement	$1{\cdot}094 \times 10^{-2}$		
Parameter identification	$1{\cdot}067 \times 10^{-2}$	36·780	− 444·702

acceleration of the experimental set-up yield results for Duffing's model parameters of $a = 1{\cdot}067 \times 10^{-2}$, $b = 36{\cdot}780$ and $c = -444{\cdot}702$.

6.2.3. *Comparison between statistically and dynamically obtained results*

The comparison of the parameters of Duffing's model are shown in Table 9. It can be seen that the values of parameter a differ the least ($-2{\cdot}53\%$). Both values of parameter a have been estimated from a measured system response, e.g., dynamically. A somewhat larger difference in values can be found with the parameter b ($-7{\cdot}69\%$). The parameter c is estimated to be negative in both cases, which is consistent and describes the degressive spring characteristic. Such a large difference is due to the lower sensitivity of Duffing's model for that particular parameter.

The comparison of the measured acceleration, the simulated acceleration based on identified parameters of Duffing's model and the simulated acceleration based on statically estimated stiffness parameters and the dynamically estimated parameter a of Duffing's model are shown in Figure 5. We can see clearly that there is no major difference between the measured response (——) and the response based on the identification procedure

(·····). The difference between the measured response and the response based on parameters that have been partially statically determined (– – –) is clearly visible in Figure 5.

Since we believe that our approach is relatively simple to implement, we also considered the simple and pragmatic approach of evaluating the system's properties by static stiffness test and by logarithmic decrement. The comparison of the approaches in Figure 5 shows that evaluating the system's properties by static stiffness test and by logarithmic decrement is just not accurate enough. In contrast, our approach gives good results in spite of its simplicity.

6.3. DISTINCTION BETWEEN THE EQUIVALENT VISCOUS AND FRICTION DAMPING

An LVDT (Linear Variable Differential Transformer) was added to the experimental set-up described in the previous sub-sections in order to provide the frictional damping and to provide a means to estimate the frictional damping from the amplitudes' decay. The LVDT's core was attached to the inertial mass by a small permanent magnet. In this way, the core's movement perpendicular to the direction of the oscillations is enabled.

The time histories were sampled with a 12 bit A/D converter and stored on a PC HDD. The sampling frequency was set at 1 kHz. A higher harmonic is present in the acceleration time history which can be seen in Figure 9. This happens because the frictional contact in LVDT (stick–slip phenomenon) triggers natural bending vibrations in the springs. The springs are modelled as massless elements of a given stiffness. Hence, the natural bending vibrations of the springs are considered as noise when identifying the parameters of Duffing's model.

The parameter d of Duffing's model was first estimated using the theory of constant amplitude decay of the displacement time series. The value was estimated as $d = 0{\cdot}084$.

The dynamically determined spring characteristic was computed by using the approach described in this paper. The acceleration time history was measured with an accelerometer glued to the inertial mass and is chosen to be the base for the reconstruction of the state space. The state space was reconstructed with the approximating cubic splines, due to the "noise" polluted time history. The parameters were identified on the first two-and-a-half cycles of the response, i.e., on the first 2·5 s of the time history. The time-window approach to identification has been adopted because of the length of the identification interval.

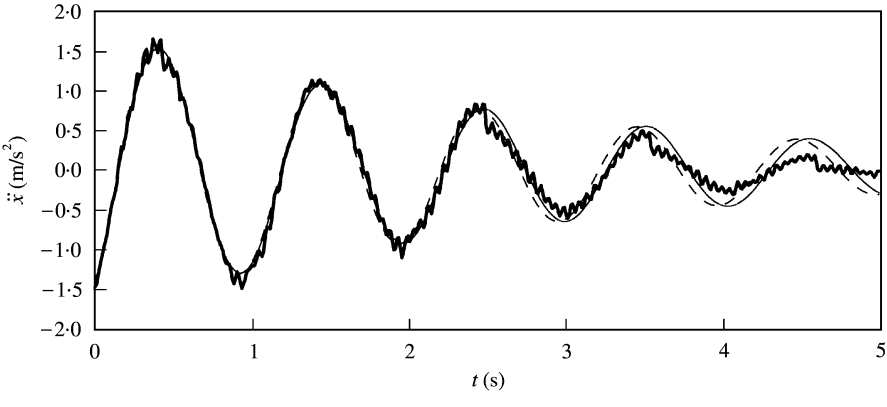

Figure 9. The comparison between measured acceleration (▬) and responses of the model 1 (——) and model 4 (– – – –).

The six different models were tested against the measured data, and so the different combinations of the viscous and frictional damping were tested. Due to fast amplitude decay, the question of the justification of the use of Duffing's model stiffness non-linearity is raised.

The models used are presented in Table 10. The model identification number is written in the first column. The second column shows the equation of motion of the model. The remaining four columns present identified values of the parameters.

The estimated value of parameter d on the basis of the amplitude decay and the identified values of the same parameter in the absence of viscous damping are in very good agreement. It can be seen that the identified values of the parameter b are very similar to the value identified without LVDT for the first three models, where the non-linearity of the stiffness is neglected. The values of the parameter b of the models 4 and 6 are about 5% higher than those identified without LVDT. This is due to the higher identified values of the parameter c. It is well-known that parameter c influences the response's frequency, which is described by parameter b, as well as amplitudes. The same is true for parameter a. The combination of parameters a and c gives rise to the value of parameter b. Model 5 is an exception, because the Coulomb model of dry friction does not influence the frequency of the response. It influences amplitudes only.

The effort of the identification approach described here, to share out the dissipated energy between the dissipation mechanisms used, is clearly visible in Table 10, models 3 and 6. The identified values of the parameter a that describe equivalent viscous damping are much bigger than the case in the previous section. The values of the parameter d are identified as being half the size of the case without viscous damping. None of the energy-dissipation models matches the real mechanisms of the energy dissipation in the system. Hence, the approach shares dissipated energy among the available energy dissipation models as best as it can. It was shown in Tables 3 and 4 that the identification approach estimates lower values of parameter d than the true values.

The comparison between the measured acceleration and the simulated accelerations based on identified parameters of the different models presented in Table 10 are shown in Figure 9, for models 1 and 4; Figure 10, for models 2 and 5; Figure 11, for models 3 and 6.

Figure 9 shows that models 1 and 4, which are without frictional damping, circumscribe the measured acceleration adequately when amplitudes are still high. Both fail to circumscribe the time history at smaller amplitudes. It is also clear that both models cannot describe the acceleration jump when the frictional force switches its direction.

Models 2 and 5 (Figure 10) which are without viscous damping, can describe the jump in acceleration, but the dissipation of energy is identified as too low.

TABLE 10

Identified values of the parameters at different models

Model	Equation of motion	a	b	c	d
1	$z + ay + bx = 0$	0·667	36·916		
2	$z + bx + d\,\mathrm{sgn}(y) = 0$		36·678		0·0836
3	$z + ay + bx + d\,\mathrm{sgn}(y) = 0$	0·398	36·831		0·0412
4	$z + ay + bx + cx^3 = 0$	0·710	38·807	−1084·119	
5	$z + bx + cx^3 + d\,\mathrm{sgn}(y) = 0$		36·721	− 702·166	0·0811
6	$z + ay + bx + cx^3 + d\,\mathrm{sgn}(y) = 0$	0·442	38·515	− 996·652	0·0386

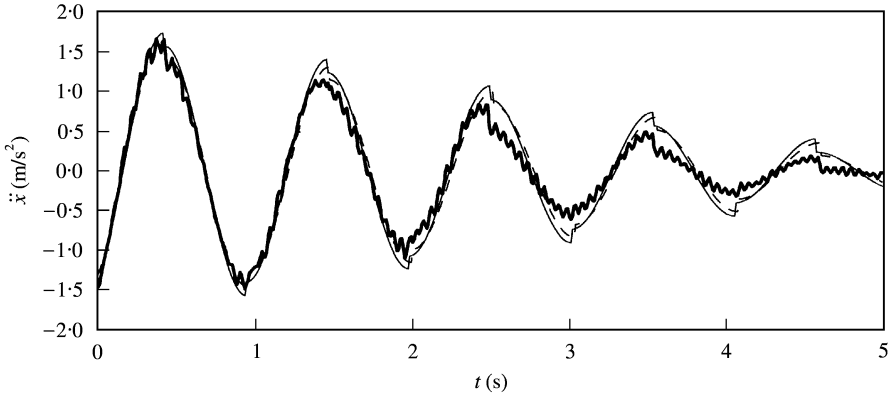

Figure 10. The comparison between measured acceleration (▬) and responses of the model 2 (——) and model 5 (– – –).

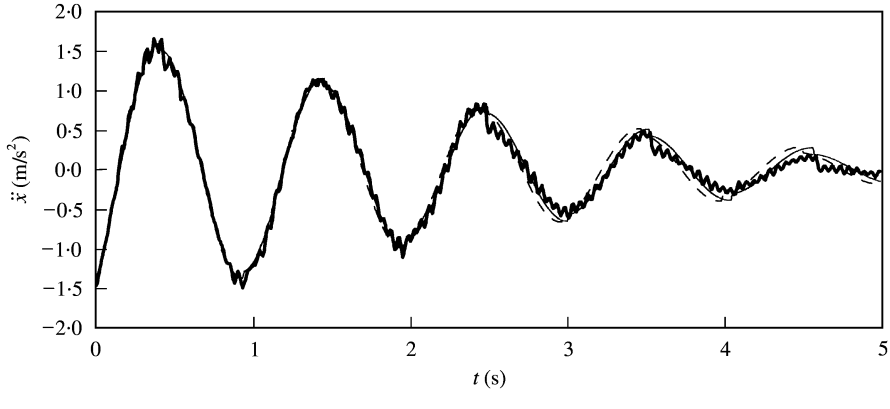

Figure 11. The comparison between measured acceleration (▬) and responses of the model 3 (——) and model 6 (– – –).

The best results are achieved when using both energy dissipation mechanisms, e.g., the viscous damping and the Coulomb model of dry friction, models 3 and 6 in Figure 11. The same figure shows that model 3, which has incorporated linear stiffness, give slightly better results than model 6 with non-linear stiffness of the spring. This is due to the fact that the amplitude decay is rapid and the non-linearity of the stiffness does not play an important role at small amplitudes. The difference is visible only in the second half of the response, where the parameters were not identified. There are practically no differences between models 3 and 6 in the first half of the response, where the amplitudes are still large and where the parameters were identified.

The second half of the response is reasonably well approximated by models 3 and 6. The approximation of the response is as good as the models of energy dissipation used will allow.

7. CONCLUSIONS

In this paper, an approach to parameter identification for the s.d.o.f. mechanical system based on measured acceleration is presented. Duffing's system with dry friction was taken

into consideration. The approach follows the concept of computing the parameters of the differential equation of motion, which can be represented as an algebraic equation if the parameters are considered to be unknowns.

The numerical experiment was carried out first. The influence of varying stiffness non-linearity on the success of the approach and the possibility of a distinction between viscous and frictional damping mechanisms was tested. The responses of Duffing's model based on the identified parameters and the responses based on the true values of the parameters are in very good agreement. The results of the approach were also compared to the results of the method proposed by Staszewski [12] and comparable results were found if the data are prepared properly for the proposed approach.

The experimental work was divided into two parts. In the first part, the spring characteristic was determined statically and dynamically using the proposed approach. The equivalent viscous damping described by parameter a was also estimated by two different methods, firstly by logarithmic decrement and secondly by our approach. It was shown that it is difficult to draw a distinction between the measured response and the response gained by our approach and that the response simulated on the basis of the static test and logarithmic decrement significantly differs from the measured time history.

In the second part of the experimental work, the success of the approach was tested on the response of a rather noisy system and the appropriate model for the frictionally damped system was determined. It is shown that the models with only one modelled mechanism of energy dissipation cannot represent the motion of the system sufficiently accurate. This can be achieved by fitting the viscous and frictional damping into the model. It was also shown that modelling of the non-linear spring stiffness is not necessary in that case, due to fast amplitude decay.

The results of the identified parameters differ somewhat from those estimated with the static test. This is due to the fact that the approach optimally, in the sense of least mean squares, fits all of the model's parameters to the measured acceleration simultaneously, which is not the case if the parameters are estimated individually with separate tests.

The spring characteristic of the system can be estimated with a static test but there is no way other than a dynamical test to estimate parameters describing the dissipation of the energy. The approach identifies the parameters of the chosen model with dynamically gained free-acceleration-response data under the working conditions. Hence, it enables the model's parameters for part of the machinery to be estimated without the need to disassemble it. In such a case, the extra tests on the part are unnecessary and this reduces the required experimental work.

The results show that the proposed approach offers parameter identification with good quality for short time series (a few cycles) using only a modest number of data points for a wide range of s.d.o.f. systems. It offers easy ways for computing the parameters and initial conditions from the free-acceleration-response data of the s.d.o.f. system. The approach is insensitive to initial conditions and only the type of equation of motion needs to be known.

REFERENCES

1. F. BADRAKHAN 1985 *Journal of Sound and Vibration* **100**, 243–255. Separation and determination of combined dampings from free vibrations.
2. H. G. NATKE and M. ZAMIROWSKI 1990 *Zeitschrift fuer angewandte Mathematik und Mechanik* **70**, 415–420. On methods of structure identification for the class of polynomials within mechanical systems.
3. C.-M. YING and B. JOSEPH 1999 *Industrial and Engineering Chemistry Research* **38**, 4712–4728. Identification of stable linear systems using polynomial kernels.

4. M. SEKAVČNIK 2000 *Journal of Mechanical Engineering* (*Strojniški vestnik*) **46**, 750–761. Analysis of turbocharger impeller vibrations.
5. Q. CHEN and G. R. TOMLINSON 1996 Parametric identification of systems with dry friction and nonlinear stiffness using a time series model. *Transactions of the American Society of Mechanical Engineers — Journal of Vibration and Acoustic* **118**, 252–263.
6. A. BOUKHRIST, G. MOUROT and J. RAGOT 1999 *International Journal of Control* **72**, 591–604. Non-linear dynamic system identification: a multi-model approach.
7. K. A. F. MOUSTAFA and H. E. EMARA-SHABAIK 2000 *Journal of Acoustic and Control* **6**, 49–60. Recursive parameter identification of a class of non-linear systems from noisy measurements.
8. H. J. RICE 1995 *Journal of Sound and Vibration* **185**, 473–481. Identification of weakly non-linear systems using equivalent linearization.
9. G.-M. LEE 1997 *Mechanical Systems and Signal Processing* **11**, 219–228. Estimation of non-linear system parameters using higher-order frequency response function.
10. M. FELDMAN 1994 *Mechanical Systems and Signal Processing* **8**, 119–127. Non-linear system vibration analysis using Hilbert transform—i. free vibration analysis method 'freevib'.
11. M. FELDMAN 1994 *Mechanical Systems and Signal Processing* **8**, 309–318. Non-linear system vibration analysis using Hilbert transform—ii. forced vibration analysis method 'forcevib'.
12. W. J. STASZEWSKI 1998 *Journal of Sound and Vibration* **214**, 639–658. Identification of non-linear systems using multi-scale ridges and skeletons of the wavelet transform.
13. S. F. MASRI, A. G. CHASSIAKOS and T. K. CAUGHEY 1993 *Transactions of the American Society of Mechanical Engineers—Journal of Applied Mechanics* **60**, 123–133. Identification of nonlinear dynamic system using neural networks.
14. A. G. CHASSIAKOS and S. F. MASRI 1996 *Mathematics and Computers in Simulation* **40**, 637–656. Identification of structural systems by neural network.
15. N. YADAIAH, N. SIVAKUMAR and B. L. DEEKSHATULU 2000 *Mathematics and Computers in Simulation* **51**, 157–167. Parameter identification via neural networks with fast convergence.
16. M. YAR and J. K. HAMMOND 1987 *Journal of Sound and Vibration* **117**, 161–172. Parameter estimation for hysteretic systems.
17. Y. Q. NI, J. M. KO and C. W. WONG 1998 *Journal of Sound and Vibration* **217**, 737–756. Identification of non-linear hysteretic isolators from periodic vibration tests.
18. A. G. CHASSIAKOS, S. F. MASRI, A. W. SMYTH and T. K. CAUGHEY 1998 *Transactions of the American Society of Mechanical Engineers—Journal of Applied Mechanics* **65**, 194–203. On-line identification of hysteretic systems.
19. A. W. SMYTH, S. F. MASRI, A. G. CHASSIAKOS and T. K. CAUGHEY 1999 *Journal of Engineering Mechanics—American Society of Civil Engineers* **125**, 133–142. On-line parametric identification of mdof nonlinear hysteretic systems.
20. N. JAKŠIĆ, M. BOLTEŽAR and A. KUHELJ 2000 in *Seventh International Conference on Recent Advances in Structural Dynamics*, (N. S. Ferguson, H. F. Wolfe, M. A. Ferman and S. A. Rizzi, editors), Vol. **2**, 951–964, 24–27 July. Southampton: Institute of Sound and Vibration Research, University of Southampton. Parameter identification of a single degree of freedom dynamical system based on phase space variables.
21. N. JAKŠIĆ, M. BOLTEŽAR and A. KUHELJ 2000 in *Slovensko društvo za mehaniko*, *Kuhljevi dnevi* 2000, *Zbornik del*, (L. Škerget, editor), Maribor, 21–22, September, 199–206. Slovensko društvo za mehaniko Identifikacija parametrov lastnega nihanja mehanskih sistemov z eno prostostno stopnjo (Parameter identification of natural vibrations of s.d.o.f. systems).
22. J. M. T. THOMPSON and H. B. STEWART 1986 *Nonlinear Dynamics and Chaos*. New York: John Wiley and Sons Ltd.; Sixth reprint edition.